

# Predictions of Light Hadronic Decays of Heavy Quarkonium $^1D_2$ States in NRQCD

Ying Fan,<sup>1,\*</sup> Zhi-Guo He,<sup>1,†</sup> Yan-Qing Ma,<sup>1,‡</sup> and Kuang-Ta Chao<sup>1,§</sup>

<sup>1</sup>*Department of Physics and State Key Laboratory of Nuclear Physics and Technology,  
Peking University, Beijing 100871, China*

(Dated: April 26, 2022)

## Abstract

The inclusive light hadronic decays of  $^1D_2$  heavy quarkonia are studied within the framework of NRQCD at the leading order in  $v$  and up to the order of  $\alpha_s^3$ . With one-loop QCD corrections, the infrared divergences and Coulomb singularities in the decay amplitudes are proved to be absorbed by the renormalization of the matrix elements of corresponding NRQCD operators, and the infrared finite short-distance coefficients are obtained through the matching calculations. By taking the factorization scale to be  $2m_Q$ , the light hadronic decay widths are estimated to be about 274, 4.7, and 8.8 KeV for the  $\eta_{c2}$ ,  $\eta_{b2}$ , and  $\eta'_{b2}$  respectively. Based on the above estimates, and using the E1 transition width and dipion transition width for the  $\eta_{c2}$  estimated elsewhere, we get the total width of  $\eta_{c2}$  to be about 660-810 KeV, and the branching ratio of the E1 transition  $\eta_{c2} \rightarrow \gamma h_c$  to be about (44-54)%, which will be useful in searching for this missing charmonium state through, e.g., the process  $\eta_{c2} \rightarrow \gamma h_c$  followed by  $h_c \rightarrow \gamma \eta_c$ .

PACS numbers: 12.38.Bx, 12.39.St, 13.20.Gd

---

\*Electronic address: ying.physics.fan@gmail.com

†Electronic address: hzgzh@gmail.com

‡Electronic address: yqma.cn@gmail.com

§Electronic address: ktchao@th.phy.pku.edu.cn

## I. INTRODUCTION

The studies of production and decay mechanisms for heavy quarkonia provide important information on both perturbative and nonperturbative QCD. Based on the nonrelativistic (NR) nature of heavy quarkonium systems, an effective field theory, the nonrelativistic QCD (NRQCD) factorization formalism was proposed by Bodwin, Braaten and Lepage in 1990s[1]. Within this framework, the inclusive decay and production of heavy quarkonium can be factorized into two parts, the short distance coefficients and the long distance matrix elements. Differing from the color-singlet model (CSM) [2], in the NRQCD factorization formalism, the heavy quark and antiquark pair annihilated or produced at short distances can be in both the color-singlet and the color-octet states with the same or different angular momentum quantum numbers [1], and the latter is known as the color-octet mechanism (COM). This mechanism has been used to remove the infrared divergences in inclusive P-wave charmonium production [3] and decay [1, 4, 5, 6] to give the infrared safe and model independent predictions.

Recently, the inclusive light hadronic decays of  $^3D_J$  charmonium states were also studied within the framework of NRQCD factorization up to order  $\alpha_s^3$ [7, 8]. The infrared divergence found in the CSM calculation [9] is removed by absorbing it into the matrix elements of the color-octet  $^3P_J$  operators. Furthermore, the new contributions at order  $\alpha_s^2$  from the color-octet  $^3P_J$  and  $^3S_1$  matrix elements enhance the decay widths of  $^3D_J$  states, and the numerical results are larger than those estimated in the CSM by several times in magnitude [8]. One can expect that a similar case will emerge in the inclusive light hadronic decay of  $^1D_2$  charmonium, namely, the  $\eta_{c2}$  state. The difference between the  $\eta_{c2}$  and  $^3D_J$  states is that there are no infrared divergences in the inclusive decay width of  $\eta_{c2}$  in the CSM up to order  $\alpha_s^2$  [10], and the numerical result is about 110 KeV [11]. However, the infrared divergence will emerge again in the decay width of  $\eta_{c2}$  in the CSM at order  $\alpha_s^3$ , which needs to be removed by invoking the color-octet mechanism, i.e. by absorbing it into the corresponding color-octet matrix elements.

On the other hand, the estimation of the inclusive light hadronic decay width of  $\eta_{c2}$  is also important phenomenologically for probing this missing charmonium state. Quark model predicts its mass within the range 3.80-3.84 GeV [12, 13], which lies between the  $D\bar{D}$  and the  $D^*\bar{D}$  thresholds. However, its odd parity ( $J^{PC} = 2^{-+}$ ) forbids the decay to  $D\bar{D}$ . As

a result, it should be a narrow state, and its main decay modes are the electric as well as hadronic transitions to lower-lying charmonium states and the inclusive light hadronic decay. Therefore, the study for the inclusive light hadronic decay of  $\eta_{c2}$  in NRQCD factorization will provide important information on searching for this state in high-energy  $p\bar{p}$  collision [14], in  $B$  decays [15], in higher charmonium transitions, and in the low-energy  $p\bar{p}$  reaction in PANDA at FAIR [16] and in  $e^+e^-$  process in BESIII at BEPC [17].

In this paper, we study the one-loop QCD corrections to light hadronic decay of  $^1D_2$  within the framework of NRQCD factorization. The paper is organized as follows: after an introduction of the NRQCD factorization formalism in Sec. II, we calculate the decay widths up to  $\mathcal{O}(\alpha_s^3)$  in perturbative QCD in Sec. III, where both the real and virtual corrections are considered. Then perturbative NRQCD is applied to obtain the imaginary parts of the forward scattering amplitudes in Sec. IV. Combined with the QCD results, the infrared divergences are either canceled or absorbed into the long distance NRQCD matrix elements, and the finite short distance coefficients are obtained. Together with the long distance matrix elements estimated by solving the operator evolution equations, the decay width is determined. The numerical results and phenomenological discussions are given in Sec. V. In the last, we will give a brief summary for our results in Sec. VI.

## II. GENERAL FORMULAS

There are four important scales in the heavy quarkonium system: the heavy quark mass  $m_Q$ , the typical momentum of the heavy quark or the inverse of the size of the bound state  $m_Q v$ <sup>a</sup>, the binding energy  $m_Q v^2$  and the QCD scale  $\Lambda_{QCD}$ , while the dynamical property of the bound state is mainly determined by the latter three scales. Thus one can choose a cutoff  $\mu_\Lambda$  with condition  $m_Q > \mu_\Lambda \gg m_Q v$  ( $m_Q v^2$ ,  $\Lambda_{QCD}$ ) to integrate out the hard scale  $m_Q$ . Expanding the nonlocal effective action in power of  $v$  and writing the result in the two-component Pauli spinor space, one then can get the effective Lagrangian for NRQCD [1]:

$$\mathcal{L}_{NRQCD} = \mathcal{L}_{light} + \mathcal{L}_{heavy} + \delta\mathcal{L}, \quad (1)$$

---

<sup>a</sup> Here,  $v$  denotes the relative velocity of the heavy quark pair in the meson frame. The average value of  $v^2$  is about 0.3 for charmonium and about 0.1 for bottomonium [1].

where the Lagrangian  $\mathcal{L}_{light}$  describes gluon and light quarks. At leading order in  $v$ , the heavy quark and antiquark are described by  $\mathcal{L}_{heavy}$ :

$$\mathcal{L}_{heavy} = \psi^\dagger (iD_t + \frac{\mathbf{D}^2}{2m_Q})\psi + \chi^\dagger (iD_t - \frac{\mathbf{D}^2}{2m_Q})\chi, \quad (2)$$

where  $\psi$  denotes the Pauli spinor field that annihilates a heavy quark,  $\chi$  denotes the Pauli spinor field that creates a heavy antiquark, and  $D_t$  and  $\mathbf{D}$  are the time and space components of the gauge-covariant derivative  $D^\mu$ , respectively. The relativistic corrections to  $\mathcal{L}_{heavy}$  are included in the term  $\delta\mathcal{L}$ . The most important correction terms for heavy quarkonium energy splitting are the bilinear ones:

$$\begin{aligned} \delta\mathcal{L}_{bilinear} = & \frac{c_1}{8m_Q^3} [\psi^\dagger (\mathbf{D}^2)^2 \psi - \chi^\dagger (\mathbf{D}^2)^2 \chi] \\ & + \frac{c_2}{8m_Q^2} [\psi^\dagger (\mathbf{D} \cdot g\mathbf{E} - g\mathbf{E} \cdot \mathbf{D}) \psi + \chi^\dagger (\mathbf{D} \cdot g\mathbf{E} - g\mathbf{E} \cdot \mathbf{D}) \chi] \\ & + \frac{c_3}{8m_Q^2} [\psi^\dagger (i\mathbf{D} \times g\mathbf{E} - g\mathbf{E} \times i\mathbf{D}) \cdot \boldsymbol{\sigma} \psi + \chi^\dagger (i\mathbf{D} \times g\mathbf{E} - g\mathbf{E} \times i\mathbf{D}) \cdot \boldsymbol{\sigma} \chi] \\ & + \frac{c_4}{2m_Q} [\psi^\dagger (g\mathbf{B} \cdot \boldsymbol{\sigma}) \psi - \chi^\dagger (g\mathbf{B} \cdot \boldsymbol{\sigma}) \chi], \end{aligned} \quad (3)$$

where  $E^i = G^{0i}$  and  $B^i = \frac{1}{2}\epsilon^{ijk}G^{jk}$  are the electric and magnetic components of the gluon field-strength tensor  $G^{\mu\nu}$ , respectively.

In the Lagrangian  $\mathcal{L}_{NRQCD}$  in (1), there are still three low-energy scales: the soft scale  $m_Q v$ , the ultrasoft scale  $m_Q v^2$  and the QCD scale  $\Lambda_{QCD}$ . The existence of multi-scales makes the power counting rules of NRQCD (the velocity scaling rules [1]) can not be homogeneous generally. More seriously, if one wants to do the NRQCD loop calculations in dimensional regularization scheme with  $\mathcal{L}_{NRQCD}$  defined in (1), one will find that the hard scale can not decouple from the loop integrals and the power counting rules are violated inevitably [18]. These problems can be solved simultaneously by the method of regions [19], which will be explained and applied in our calculations in Sec. IV.

To reproduce the annihilation contribution to a low-energy  $Q\bar{Q} \rightarrow Q\bar{Q}$  scattering amplitude in NRQCD, local four-fermion operators in  $\delta\mathcal{L}$  are needed, which have the general form [1]

$$\delta\mathcal{L}_{4-fermion} = \sum_n \frac{f_n(\mu_\Lambda)}{m_Q^{d_n-4}} \mathcal{O}_n(\mu_\Lambda). \quad (4)$$

where  $\mathcal{O}_n$  denotes regularized local four-fermion operators, such as  $\psi^\dagger \chi \chi^\dagger \psi$ , and  $d_n$  is the naive scaling dimension of the operator. The dependence on cutoff  $\mu_\Lambda$  of the operator  $\mathcal{O}_n$

is canceled by that of scaleless coefficient  $f_n(\mu_\Lambda)$ , which can be computed by matching the full QCD onto the NRQCD as perturbation series in  $\alpha_s$ .

In NR theory, the width of heavy quarkonium  $H$  is  $-2$  times the imaginary part of the energy of the state, thus one has [1]

$$\Gamma(H \rightarrow LH) = 2\text{Im}\langle H | \delta\mathcal{L}_{4\text{-fermion}} | H \rangle = \sum_n \frac{2\text{Im}f_n(\mu_\Lambda)}{m_Q^{d_n-4}} \langle H | \mathcal{O}_n(\mu_\Lambda) | H \rangle, \quad (5)$$

where  $LH$  represents all possible light hadronic final states, and the operator  $\mathcal{O}_n$  here and afterward only denotes the one relevant to the strong annihilation of  $Q\bar{Q}$ . The NR normalization has been applied for the state  $|H\rangle$  in (5).

In order to calculate the coefficients of four-fermion operators in (5), the equivalence of full QCD and NRQCD at long distance is exploited. Since in construction, the coefficient  $f_n$  is of short-distance nature and is independent on the long distance asymptotic state, one can get it by replacing the state  $|H\rangle$  by the on-shell heavy quark pair state  $|Q\bar{Q}\rangle$  with small relative momentum and matching the forward scattering amplitude of  $Q\bar{Q} \rightarrow Q\bar{Q}$  in full QCD onto that of NRQCD perturbatively. The matching condition is written as [1]

$$\mathcal{A}(Q\bar{Q} \rightarrow Q\bar{Q}) \Big|_{\text{pert QCD}} = \sum_n \frac{f_n(\mu_\Lambda)}{m_Q^{d_n-4}} \langle Q\bar{Q} | \mathcal{O}_n(\mu_\Lambda) | Q\bar{Q} \rangle \Big|_{\text{pert NRQCD}}. \quad (6)$$

Since we only need the imaginary parts of the coefficients, optical theorem can be used to simplify the matching calculations.

The physical  $^1D_2$  state can be expanded in powers of  $v$  in the Fock space:

$$|^1D_2\rangle = \mathcal{O}(1)|Q\bar{Q}(^1D_2^{[1]})\rangle + \mathcal{O}(v)|Q\bar{Q}(^1P_1^{[8]})\rangle + \mathcal{O}(v^2)|Q\bar{Q}(^1S_0^{[1,8]})\rangle + \mathcal{O}(v^3), \quad (7)$$

where the superindices [1] and [8] denote the color-singlet and color-octet, respectively. The contributions from the P-wave and S-wave Fock states to the annihilation rate of  $^1D_2$  are at the same order of  $v^2$  as that from the D-wave state, because their relevant operators scale  $v^{-2}$  and  $v^{-4}$  relative to  $\mathcal{O}_1(^1D_2)$ , as can be seen later. Other Fock states contribute at higher order of  $v^2$ . Therefore the light hadronic decay width of  $^1D_2$  at leading order in  $v^2$  can be described in NRQCD factorization framework as follows:

$$\begin{aligned} \Gamma(^1D_2 \rightarrow LH) = & 2 \text{Im}f(^1D_2^{[1]}) \frac{\langle ^1D_2 | \mathcal{O}_1(^1D_2) | ^1D_2 \rangle}{m_Q^6} + 2\text{Im}f(^1P_1^{[8]}) \frac{\langle ^1D_2 | \mathcal{O}_8(^1P_1) | ^1D_2 \rangle}{m_Q^4} + \\ & 2 \text{Im}f(^1S_0^{[8]}) \frac{\langle ^1D_2 | \mathcal{O}_8(^1S_0) | ^1D_2 \rangle}{m_Q^2} + 2\text{Im}f(^1S_0^{[1]}) \frac{\langle ^1D_2 | \mathcal{O}_1(^1S_0) | ^1D_2 \rangle}{m_Q^2}, \end{aligned} \quad (8)$$

where the four-fermion operators are [21]:

$$\begin{aligned}
\mathcal{O}_1(^1S_0) &= \frac{1}{2N_c} \psi^\dagger \chi \chi^\dagger \psi, \\
\mathcal{O}_8(^1S_0) &= \psi^\dagger T^a \chi \chi^\dagger T^a \psi, \\
\mathcal{O}_8(^1P_1) &= \psi^\dagger \left(-\frac{i}{2} \overleftrightarrow{\mathbf{D}}\right) T^a \chi \cdot \chi^\dagger \left(-\frac{i}{2} \overleftrightarrow{\mathbf{D}}\right) T^a \psi, \\
\mathcal{O}_1(^1D_2) &= \frac{1}{2N_c} \psi^\dagger S^{ij} \chi \chi^\dagger S^{ij} \psi,
\end{aligned} \tag{9}$$

where  $\overleftrightarrow{\mathbf{D}} = \overrightarrow{\mathbf{D}} - \overleftarrow{\mathbf{D}}$  and  $S^{ij} = (-\frac{i}{2})^2 (\overleftrightarrow{\mathbf{D}}^i \overleftrightarrow{\mathbf{D}}^j - \frac{1}{3} \overleftrightarrow{\mathbf{D}}^2 \delta^{ij})$ . Since  $\mathbf{D}^2/m_Q^2$  scales as  $v^2$ , it can be ensured that the four terms in (8) are at the same order of  $v$ .

The coefficients in (8) can be obtained by applying the matching conditions (6) to appropriate  $Q\bar{Q}$  configurations. To subtract the full QCD amplitude of  $Q\bar{Q}$  state of particular angular momentum, the covariant projection method is adopted. In practice, the optical theorem can relate the imaginary part of the QCD amplitude  $\mathcal{A}$  in (6) to the parton level decay width [20, 21]

$$\Gamma(Q\bar{Q}[n] \rightarrow LFs) = \frac{1}{2M} \langle Q\bar{Q}[n] | \mathcal{O}[n] | Q\bar{Q}[n] \rangle_{NR}^{LO} \overline{\sum} \int |\mathcal{M}(Q\bar{Q}[n] \rightarrow LFs)|^2 d\Phi, \tag{10}$$

where  $LFs$  denote the gluons or light quarks and  $[n]$  denotes the configuration of the  $Q\bar{Q}$ . The state  $|Q\bar{Q}[n]\rangle$  has been normalized relativistically as one composite state with mass  $M = 2E_Q$ , except that in the matrix element in (10), where the state is normalized non-relativistically to match the results in perturbative NRQCD conveniently. The super-index  $LO$  of the matrix element means that it is evaluated at tree level, and we always use the abbreviation  $\langle \mathcal{O}[n] \rangle_{LO}$  to represent it in our calculations. Moreover, the summation/average of the color and polarization for the final/initial state has been implied by the symbol  $\overline{\sum}$ .

For spin-singlet states with  $L = 0, L = 1$  and  $L = 2$ , the amplitudes  $\mathcal{M}$  defined in (10) are given by [20]

$$\begin{aligned}
\mathcal{M}((Q\bar{Q})_{1S_0}^{[1,8]} \rightarrow LFs) &= \sqrt{\frac{2}{M}} Tr[\mathcal{C}^{[1,8]} \Pi^0 \mathcal{M}^{am}]|_{q=0}, \\
\mathcal{M}((Q\bar{Q})_{1P_1}^{[8]} \rightarrow LFs) &= \epsilon_\alpha^{[P]} \sqrt{\frac{2}{M}} \frac{d}{dq_\alpha} Tr[\mathcal{C}^{[8]} \Pi^0 \mathcal{M}^{am}]|_{q=0}, \\
\mathcal{M}((Q\bar{Q})_{1D_2}^{[1]} \rightarrow LFs) &= \frac{1}{2} \epsilon_{\alpha\beta}^{[D]} \sqrt{\frac{2}{M}} \frac{d^2}{dq_\alpha dq_\beta} Tr[\mathcal{C}^{[1]} \Pi^0 \mathcal{M}^{am}]|_{q=0},
\end{aligned} \tag{11}$$

where  $\mathcal{M}^{am}$  denotes the parton-level amplitude amputated of the heavy quark spinors, and  $\epsilon_\alpha^{[P]}$  and  $\epsilon_{\alpha\beta}^{[D]}$  are the polarization tensors for  $L = P, D$  states respectively. The factor

$\sqrt{\frac{2}{M}} = \frac{\sqrt{2M}}{\sqrt{2E_Q}\sqrt{2E_Q}}$  comes from the normalization of the composite state  $|Q\bar{Q}[n]\rangle$ . For color singlet and octet states, the color projectors are  $\mathcal{C}^{[1]} = \frac{\delta_{ij}}{\sqrt{N_c}}$  and  $\mathcal{C}^{[8]} = \sqrt{2}(T_a)_{ij}$  respectively [20]. The covariant spin-singlet projector  $\Pi^0$  in (11) is defined by

$$\Pi^0 = \sum_{s\bar{s}} u(s)\bar{v}(\bar{s})\langle \frac{1}{2}, s; \frac{1}{2}, \bar{s} | 0, 0 \rangle. \quad (12)$$

The explicit form of  $\Pi^0$  in D dimensions will be discussed in the latter subsection.

The sums over polarization tensors for  $\epsilon_\alpha^{[P]}$  and  $\epsilon_{\alpha\beta}^{[D]}$  in D dimensions are:

$$\sum_{J_z} \epsilon_\alpha^{[P]} \epsilon_{\alpha'}^{[P]*} = \Pi_{\alpha\alpha'}, \quad (13a)$$

$$\sum_{J_z} \epsilon_{\alpha\beta}^{[D]} \epsilon_{\alpha'\beta'}^{[D]*} = \frac{1}{2}(\Pi_{\alpha\alpha'}\Pi_{\beta\beta'} + \Pi_{\alpha\beta'}\Pi_{\alpha'\beta}) - \frac{1}{D-1}\Pi_{\alpha\beta}\Pi_{\alpha'\beta'}. \quad (13b)$$

Here  $\Pi_{\alpha\alpha'}$  is defined as

$$\Pi_{\alpha\alpha'} = -g_{\alpha\alpha'} + \frac{P_\alpha P_{\alpha'}}{M^2}, \quad (14)$$

where  $P$  is the total momentum of  $Q\bar{Q}$ , and  $P^2 = M^2 = 4E_Q^2$ .

Needless to say, the final result should be independent on the normalization convention of the  $Q\bar{Q}$  state. If one wants to apply NR normalization thoroughly in the calculations, one needs to eliminate the factors  $1/(2M)$  in (10) and  $\sqrt{2/M}$  in (11), and then to replace the covariant spinors in (12) with the NR ones with the normalization condition:  $u^\dagger u = v^\dagger v = 1$ .

### A. Discussions on $\gamma^5$ scheme and projection operator

We will do our calculations in dimensional regularization scheme both for QCD and NRQCD. Since we are only dealing with the spin-singlet Fock states, there will be the problem of definition of  $\gamma^5$  in D dimensions. In our calculation, the 't Hooft-Veltman (HV) scheme[20, 22] is introduced:

$$\begin{aligned} \{\gamma^5, \gamma^\mu\} &= 0, \quad \mu = 0, 1, 2, 3 \\ [\gamma^5, \gamma^\mu] &= 0, \quad \mu = 4, \dots, D-1. \end{aligned} \quad (15)$$

And the  $\gamma^5$  matrix can be represented as [23]:

$$\gamma^5 = -\frac{i}{4!} \epsilon^{\mu\nu\rho\sigma} \gamma_\mu \gamma_\nu \gamma_\rho \gamma_\sigma. \quad (16)$$

The calculation involving  $\gamma^5$  is carried out in D dimensions, where  $\epsilon^{\mu\nu\rho\sigma}$  and  $\gamma^\mu$  are all defined in D dimensions. Other prescriptions may be found in literatures [24, 25, 26, 27].

In four dimensions, the covariant spin-singlet projector  $\Pi^0$  defined in (12) can be given by (see, e.g., [28])

$$\Pi^0 = \frac{1}{2\sqrt{2}(E_Q + m_Q)} \left( \frac{\not{P}}{2} + \not{q} + m_Q \right) \frac{(\not{P} + M)}{M} \gamma^5 \left( \frac{\not{P}}{2} - \not{q} - m_Q \right), \quad (17)$$

where  $q$  is half of the relative momentum of the heavy quark pair. The form in (17) can not keep **C** parity conservation in D dimensions because  $(\not{P} + M)\gamma^5$  can not keep an invariant form under charge conjugation transformation in  $D \neq 4$  dimensions in the HV scheme, which can be easily seen by applying (15). This problem can be solved by replacing it by the following two operators. For spin singlet states the spin projectors of incoming heavy quark pairs at any order in  $v^2$  are given by

$$\Pi^0 = \frac{1}{2\sqrt{2}(E_Q + m_Q)} \left( \frac{\not{P}}{2} + \not{q} + m_Q \right) \frac{[(\not{P} + M)\gamma^5 + \gamma^5(-\not{P} + M)]}{2M} \left( \frac{\not{P}}{2} - \not{q} - m_Q \right) \quad (18)$$

from [29] and

$$\Pi^0 = \frac{1}{2\sqrt{2}(E_Q + m_Q)} \left( \frac{\not{P}}{2} + \not{q} + m_Q \right) \frac{(\not{P} + M)\gamma^5(-\not{P} + M)}{2M^2} \left( \frac{\not{P}}{2} - \not{q} - m_Q \right) \quad (19)$$

from [30]. The above two projection operators both give correct results and keep **C** parity conservation.

### III. FULL QCD CALCULATION

In this section, we calculate the imaginary part of  $Q\bar{Q}$  forward scattering amplitude, or equivalently, the parton-level decay width  $\Gamma$  defined in (10). In the calculation, we use **FeynArts** [31] to generate the Feynman diagrams and amplitudes and **FeynCalc** [32] for the tensor reduction. We regularize the ultraviolet(UV) and infrared(IR) divergence in dimensional regularization scheme and extend the covariant projection method into  $D = 4 - 2\epsilon$  dimensions as has been mentioned.

The leading order subprocesses in  $\alpha_s$  are the annihilations of  $Q\bar{Q}[n]$  into two gluons, where  $n$  can be any configurations of the Fock states listed in (7). The Feynman diagrams at LO of  $\alpha_s$  are shown in Fig. 1. And the results in D dimensions are



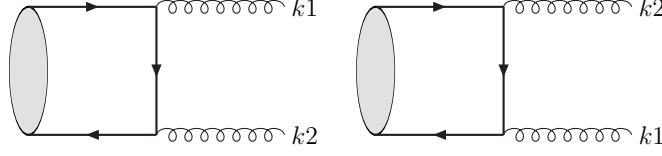


FIG. 1: Feynman diagrams for  $^1L_J^{[1,8]} \rightarrow gg$

$$\begin{aligned}
\Gamma_{\text{Born}}(^1S_0^{[1]} \rightarrow gg) &= \frac{C_F \alpha_s^2 16\pi^2}{m_Q^2} \Phi_2(1-\epsilon)(1-2\epsilon) \langle \mathcal{O}(^1S_0^{[1]}) \rangle_{LO}, \\
\Gamma_{\text{Born}}(^1S_0^{[8]} \rightarrow gg) &= \frac{B_F \alpha_s^2 16\pi^2}{m_Q^2} \Phi_2(1-\epsilon)(1-2\epsilon) \langle \mathcal{O}(^1S_0^{[8]}) \rangle_{LO}, \\
\Gamma_{\text{Born}}(^1P_1^{[8]} \rightarrow gg) &= \frac{C_A \alpha_s^2 4\pi^2}{m_Q^4} \Phi_2 \frac{(1-\epsilon)(1-2\epsilon)}{3-2\epsilon} \langle \mathcal{O}(^1P_1^{[8]}) \rangle_{LO}, \\
\Gamma_{\text{Born}}(^1D_2^{[1]} \rightarrow gg) &= \frac{C_F \alpha_s^2 4\pi^2}{m_Q^6} \Phi_2 \frac{(1-2\epsilon)(6\epsilon^2 - 15\epsilon + 8)}{4\epsilon^2 - 16\epsilon + 15} \langle \mathcal{O}(^1D_2^{[1]}) \rangle_{LO}, \quad (20)
\end{aligned}$$

where  $B_F = \frac{N_c^2 - 4}{4N_c} = \frac{5}{12}$  and  $\Phi_{(2)}$  is the two-body phase space in D dimensions:  $\frac{1}{8\pi} \frac{\Gamma(1-\epsilon)}{\Gamma(2-2\epsilon)} (\frac{\pi}{m_Q^2})^\epsilon$ . The first three results in (20) are consistent with those in Ref. [20, 21]. At the Born level, there are no IR divergences in the results since both the two gluons should be hard in the rest frame of  $Q\bar{Q}$ .

### A. Real Corrections

The real corrections to Born level subprocesses include the decays into  $ggg$  and  $q\bar{q}g$  final states. The corresponding Feynman diagrams are shown in Fig. 2 and Fig. 3. For simplicity, unphysical polarization summation is used for final state gluons, so diagrams with ghosts in the final states must be included in calculation when three gluon vertex appears, in order to cancel the non-physical degrees of freedom to keep the full results gauge invariant.

#### 1. $(Q\bar{Q})_{^1L_J^{[1,8]}} \rightarrow ggg$

Our results of S-wave configurations agree with those in [20, 21] and are listed below:

$$\begin{aligned}
\Gamma(^1S_0^{[1]} \rightarrow ggg) &= \frac{C_A \alpha_s}{\pi} \Gamma_{\text{Born}}(^1S_0^{[1]} \rightarrow gg) f_\epsilon(M^2) \left( \frac{1}{\epsilon^2} + \frac{11}{6\epsilon} + \frac{181}{18} - \frac{23}{24}\pi^2 \right), \\
\Gamma(^1S_0^{[8]} \rightarrow ggg) &= \frac{C_A \alpha_s}{\pi} \Gamma_{\text{Born}}(^1S_0^{[8]} \rightarrow gg) f_\epsilon(M^2) \left( \frac{1}{\epsilon^2} + \frac{7}{3\epsilon} + \frac{104}{9} - \pi^2 \right), \quad (21)
\end{aligned}$$

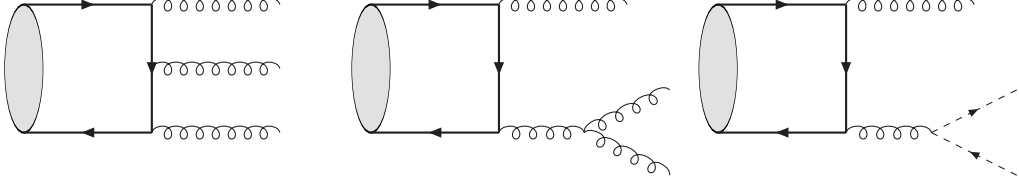


FIG. 2: Feynman diagrams for  $^1L_J^{[1,8]} \rightarrow ggg$

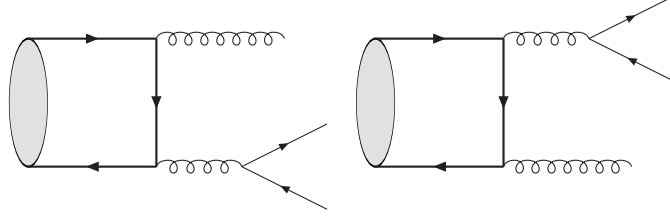


FIG. 3: Feynman diagrams for  $^1L_J^{[1,8]} \rightarrow q\bar{q}g$

where  $f_\epsilon(M^2) = (\frac{4\pi\mu^2}{M^2})^\epsilon \Gamma(1 + \epsilon)$ . The D-dimension P and D-wave results are:

$$\begin{aligned}\Gamma(^1P_1^{[8]} \rightarrow ggg) &= \frac{C_A \alpha_s}{\pi} \Gamma_{\text{Born}}(^1P_1^{[8]} \rightarrow gg) f_\epsilon(M^2) \left( \frac{1}{\epsilon^2} + \frac{71}{27\epsilon} + \frac{7(-168 + 25\pi^2)}{162} \right), \\ \Gamma(^1D_2^{[1]} \rightarrow ggg) &= \frac{C_A \alpha_s}{\pi} \Gamma_{\text{Born}}(^1D_2^{[1]} \rightarrow gg) f_\epsilon(M^2) \left( \frac{1}{\epsilon^2} + \frac{3}{\epsilon} + \frac{7027}{144} - \frac{277}{64} \pi^2 \right).\end{aligned}\quad (22)$$

Both soft and collinear IR divergences are there in the results in (21) and (22), and the square pole  $1/\epsilon^2$  comes from the overlap of the soft and the collinear regions.

## 2. $(Q\bar{Q})_{^1L_J^{[1,8]}} \rightarrow q\bar{q}g$

Another subprocess of light hadronic decay is to  $q\bar{q}g$  final states, and only two graphs make contribution to this subprocess (shown in Fig. 3).

We get the following results:

$$\begin{aligned}\Gamma(^1S_0^{[1]} \rightarrow q\bar{q}g) &= N_f \Gamma_{\text{Born}}(^1S_0^{[1]} \rightarrow gg) \frac{\alpha_s f_\epsilon(M^2)}{\pi K} T_F \left( -\frac{2}{3\epsilon} - \frac{16}{9} \right), \\ \Gamma(^1S_0^{[8]} \rightarrow q\bar{q}g) &= N_f \Gamma_{\text{Born}}(^1S_0^{[8]} \rightarrow gg) \frac{\alpha_s f_\epsilon(M^2)}{\pi K} T_F \left( -\frac{2}{3\epsilon} - \frac{16}{9} \right), \\ \Gamma(^1P_1^{[8]} \rightarrow q\bar{q}g) &= N_f \Gamma_{\text{Born}}(^1P_1^{[8]} \rightarrow gg) \frac{\alpha_s f_\epsilon(M^2)}{\pi K} T_F \left( -\frac{2}{3\epsilon} - \frac{16}{9} \right), \\ \Gamma(^1D_2^{[1]} \rightarrow q\bar{q}g) &= N_f \Gamma_{\text{Born}}(^1D_2^{[1]} \rightarrow gg) \frac{\alpha_s f_\epsilon(M^2)}{\pi K} T_F \left( -\frac{2}{3\epsilon} - \frac{16}{9} \right),\end{aligned}\quad (23)$$

where  $N_f$  is the number of light flavor quarks.  $N_f = 3$  and 4 for charmonium and bottomonium respectively.  $T_F = \frac{1}{2}$ ,  $K = \Gamma(1 + \epsilon)\Gamma(1 - \epsilon) \simeq 1 + \epsilon^2 \frac{\pi^2}{6}$  and the S-wave results agree with [20, 21].

There are only single poles of  $\epsilon$  in the results in (23) and they can be identified as collinear ones. The absence of the soft IR divergence can be seen from the diagrams in Fig. 3. When the momentum of the real gluon goes to zero, it will decouple from the quark line as an eikonal factor [21], then the results will be zero since  $Q\bar{Q}$  in spin-singlet can not couple to one virtual gluon.

As will be seen later, the collinear divergences and partial soft IR ones in (21), (22) and (23) are canceled by the virtual corrections to the Born level decay width. The remaining soft IR divergences are those in  $\Gamma(^1P_1^{[8]} \rightarrow ggg)$  and  $\Gamma(^1D_2^{[1]} \rightarrow ggg)$  from the first diagram in Fig. 2, which will be absorbed in the renormalization of the operators  $\mathcal{O}_{1,8}(^1S_0)$  and  $\mathcal{O}_8(^1P_1)$  in perturbative NRQCD. These are just the general results of the so-called topological factorization discussed in [1].

## B. Virtual Corrections

There are 23 virtual correction diagrams, including counter-term diagrams, divided into 9 groups. Representative Feynman diagrams of each class are shown in Fig. 4. And the others can be found through reversing the arrows on the quark lines or exchanging the final state gluons. UV divergences are removed by renormalization. The definitions of the renormalization constant of QCD gauge coupling constant  $g_s = \sqrt{4\pi\alpha_s}$ , heavy quark mass  $m_Q$ , heavy quark field  $\psi_Q$ , light quark field  $\psi_q$  and gluon field  $A_\mu$  are:

$$g_s^0 = Z_g g_s, \quad m_Q^0 = Z_{m_Q} m_Q, \quad \psi_Q^0 = \sqrt{Z_{2Q}} \psi_Q, \quad \psi_q^0 = \sqrt{Z_{2q}} \psi_q, \quad A_\mu^0 = \sqrt{Z_3} A_\mu, \quad (24)$$

where the superscript 0 labels bare quantities, and  $Z_i = 1 + \delta Z_i$ . The renormalized constant  $Z_g$  is defined by minimal-subtraction ( $\overline{MS}$ ) scheme, and the others by the on-mass-shell

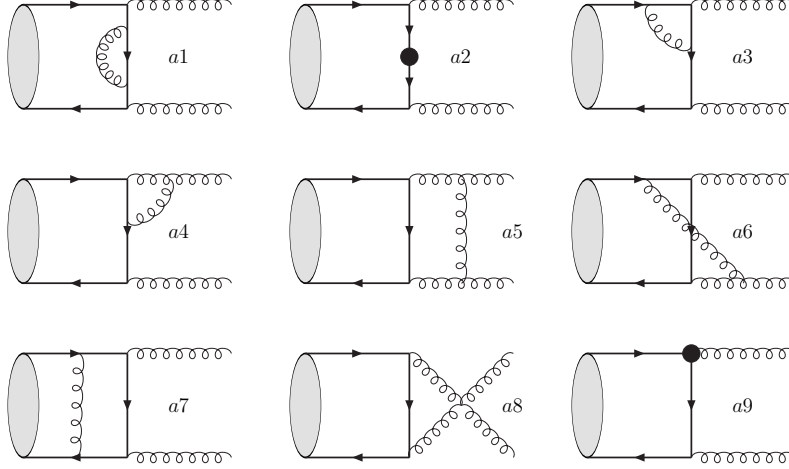


FIG. 4: One-loop Feynman diagrams for  $(Q\bar{Q})_{1L_J^{[1,8]}} \rightarrow gg$

( $OS$ ) scheme, similar to that in [33]. Then the results are:

$$\begin{aligned}
\delta Z_{2Q}^{OS} &= -C_F \frac{\alpha_s}{4\pi} f_\epsilon(M^2) \left( \frac{1}{\epsilon_{UV}} + \frac{2}{\epsilon} + 6 \ln(2) + 4 \right), \\
\delta Z_{2q}^{OS} &= -C_F \frac{\alpha_s}{4\pi} f_\epsilon(M^2) \left( \frac{1}{\epsilon_{UV}} - \frac{1}{\epsilon} \right), \\
\delta Z_3^{OS} &= (b_0 - C_A) \frac{\alpha_s}{4\pi} f_\epsilon(M^2) \left( \frac{2}{\epsilon_{UV}} - \frac{2}{\epsilon} \right), \\
\delta Z_{mQ}^{OS} &= -3C_F \frac{\alpha_s}{4\pi} f_\epsilon(M^2) \left( \frac{1}{\epsilon_{UV}} + 2 \ln(2) + \frac{4}{3} \right), \\
\delta Z_g^{\overline{MS}} &= -b_0 \frac{\alpha_s}{4\pi} f_\epsilon(M^2) \left( \frac{1}{\epsilon_{UV}} - \ln\left(\frac{\mu^2}{4m_Q^2}\right) \right),
\end{aligned} \tag{25}$$

where  $b_0 = \frac{11C_A}{6} - \frac{N_f}{3}$ .

We calculate diagrams one by one and summarize the results in the following form:

$$\Gamma(1L_J^{[1,8]} \rightarrow gg)_{VC} = \Gamma(1L_J^{[1,8]} \rightarrow gg)_{\text{Born}} \frac{\alpha_s}{\pi} f_\epsilon(M^2) \sum_k \mathcal{D}_k, \tag{26}$$

where the results of  $\mathcal{D}_k$  are listed in Table I-IV. We add the counter-term diagrams with the corresponding self-energy and vertex diagrams to show the explicit cancelation of the UV divergence. There are still IR divergences left, which will be canceled by those in the real corrections as we have mentioned. There are also the well-known Coulomb singularities, which have been regularized by the relative velocity  $v$ , in Table I-IV. These singularities can be absorbed by the corresponding matrix element through the matching condition (6).

TABLE I: Virtual corrections to  $(Q\bar{Q})_{1S_0^{[1]}} \rightarrow gg$ .

Diag.	$\mathcal{D}_k$
a1+a2	$C_F(\frac{1}{\epsilon} + 1 + 6 \ln 2)$
a3+a4+a9	$-\frac{C_A}{2\epsilon^2} + \frac{1}{\epsilon}(-2C_F - b_0 + \frac{C_A}{2}) + b_0 \ln \frac{\mu^2}{4m_Q^2} + C_F(-8 \ln 2 - 4 + \frac{\pi^2}{4}) - \frac{C_A}{2}(-4 + \frac{\pi^2}{12})$
a5	$C_A(-\frac{1}{\epsilon^2} - \frac{1}{\epsilon} - 2 + 2 \ln 2 + \frac{2}{3}\pi^2)$
a6	$\frac{1}{2}C_A(\frac{1}{\epsilon^2} + \frac{1}{\epsilon} + 2 - 4 \ln 2 - \frac{5}{12}\pi^2)$
a7	$C_F(\frac{\pi^2}{2v} + \frac{1}{\epsilon} - 2 + 2 \ln 2)$
a8	0

 TABLE II: Virtual corrections to  $(Q\bar{Q})_{1S_0^{[8]}} \rightarrow gg$ .

Diag.	$\mathcal{D}_k$
a1+a2	$C_F(\frac{1}{\epsilon} + 1 + 6 \ln 2)$
a3+a4+a9	$-\frac{C_A}{2\epsilon^2} + \frac{1}{\epsilon}(-2C_F - b_0 + \frac{C_A}{2}) + b_0 \ln \frac{\mu^2}{4m_Q^2} + C_F(-8 \ln 2 - 4 + \frac{\pi^2}{4}) - \frac{C_A}{2}(-4 + \frac{\pi^2}{12})$
a5	$\frac{1}{2}C_A(-\frac{1}{\epsilon^2} - \frac{1}{\epsilon} - 2 + 2 \ln 2 + \frac{2}{3}\pi^2)$
a6	0
a7	$(C_F - \frac{1}{2}C_A)(\frac{\pi^2}{2v} + \frac{1}{\epsilon} - 2 + 2 \ln 2)$
a8	0

### C. Summary of the QCD results

Combining the real and virtual correction results together and translating the parton-level decay width back to the imaginary part of the forward scattering amplitude, we get

TABLE III: Virtual corrections to  $(Q\bar{Q})_{1P_1^{[8]}} \rightarrow gg$ .

Diag.	$\mathcal{D}_k$
a1+a2	$C_F(\frac{1}{\epsilon} - 3 + 10 \ln 2)$
a3+a4+a9	$-\frac{C_A}{2\epsilon^2} - \frac{1}{\epsilon}(2C_F + b_0 + \frac{C_A}{2}) + b_0 \ln \frac{\mu^2}{4m_Q^2} + C_F(\frac{\pi^2}{2} - 16 \ln 2) - \frac{C_A}{2}(-6 + \frac{\pi^2}{3} + 2 \ln 2)$
a5	$\frac{1}{2}C_A(-\frac{1}{\epsilon^2} - \frac{1}{\epsilon} - 5 + \frac{2}{3}\pi^2 + 5 \ln 2)$
a6	0
a7	$(C_F - \frac{1}{2}C_A)(\frac{\pi^2}{2v} + \frac{1}{\epsilon} - 2 + 2 \ln 2)$
a8	$C_A(-\frac{1}{2} + \frac{\ln 2}{2})$

 TABLE IV: Virtual corrections to  $(Q\bar{Q})_{1D_2^{[1]}} \rightarrow gg$ .

Diag.	$\mathcal{D}_k$
a1+a2	$C_F(\frac{1}{\epsilon} - 10 + 22 \ln 2)$
a3+a4+a9	$-\frac{C_A}{2\epsilon^2} - \frac{1}{\epsilon}(2C_F + b_0 + C_A) + b_0 \ln \frac{\mu^2}{4m_Q^2} + C_F(10 + \frac{3}{4}\pi^2 - 38 \ln 2) - \frac{C_A}{2}(-\frac{15}{8} + \frac{7}{12}\pi^2 + 2 \ln 2)$
a5	$C_A(-\frac{1}{\epsilon^2} - \frac{1}{\epsilon} - 8 + \frac{2}{3}\pi^2 + 12 \ln 2)$
a6	$\frac{1}{2}C_A(\frac{1}{\epsilon^2} + \frac{69}{8} - \frac{7}{6}\pi^2 - 16 \ln 2)$
a7	$C_F(\frac{\pi^2}{2v} + \frac{1}{\epsilon} - 2 + 4 \ln 2)$
a8	0

the full QCD results up to  $\mathcal{O}(\alpha_s^3)$ :

$$\begin{aligned}
 (2\text{Im}\mathcal{A}(Q\bar{Q}[^1S_0^{[1]}] \rightarrow Q\bar{Q}[^1S_0^{[1]}])) \Big|_{\text{pert QCD}} &= \left\{ \frac{8\pi\alpha_s^2}{3m_Q^2} \left(1 + \frac{2\pi\alpha_s}{3v}\right) + \frac{\alpha_s^3}{27m_Q^2} [4(477 - 16N_f) \right. \\
 &\quad \left. + 12(33 - 2N_f) \ln \frac{\mu^2}{4m_Q^2} - 93\pi^2] \right\} \langle \mathcal{O}(^1S_0^{[1]}) \rangle_{LO},
 \end{aligned}
 \tag{27a}$$

$$\begin{aligned}
 (2\text{Im}\mathcal{A}(Q\bar{Q}[^1S_0^{[8]}] \rightarrow Q\bar{Q}[^1S_0^{[8]}])) \Big|_{\text{pert QCD}} &= \left\{ \frac{5\pi\alpha_s^2}{6m_Q^2} \left(1 - \frac{\pi\alpha_s}{12v}\right) + \frac{5\alpha_s^3}{432m_Q^2} [16(153 - 4N_f) \right. \\
 &\quad \left. + 12(33 - 2N_f) \ln \frac{\mu^2}{4m_Q^2} - 129\pi^2] \right\} \langle \mathcal{O}(^1S_0^{[8]}) \rangle_{LO},
 \end{aligned}
 \tag{27b}$$

$$\begin{aligned}
(2\text{Im}\mathcal{A}(Q\bar{Q}[^1P_1^{[8]}] \rightarrow Q\bar{Q}[^1P_1^{[8]}]))\Big|_{\text{pert QCD}} &= \left\{ \frac{\pi\alpha_s^2}{2m_Q^4} \left(1 - \frac{\pi\alpha_s}{12v}\right) - \frac{19\alpha_s^3}{18m_Q^4} \left[\frac{1}{\epsilon} - \gamma_E + \ln(4\pi)\right] \right. \\
&\quad \left. + \frac{\alpha_s^3 [2(3(-8N_f - 21\ln(2) - 229) + 119\pi^2) - 3(6N_f - 61)\ln(\frac{\mu^2}{4m_Q^2})]}{108m_Q^4} \right\} \langle \mathcal{O}(^1P_1^{[8]}) \rangle_{LO},
\end{aligned} \tag{27c}$$

$$\begin{aligned}
(2\text{Im}\mathcal{A}(Q\bar{Q}[^1D_2^{[1]}] \rightarrow Q\bar{Q}[^1D_2^{[1]}]))\Big|_{\text{pert QCD}} &= \left\{ \frac{16\pi\alpha_s^2}{45m_Q^6} \left(1 + \frac{2\pi\alpha_s}{3v}\right) - \frac{8\alpha_s^3}{9m_Q^6} \left[\frac{1}{\epsilon} - \gamma_E + \ln(4\pi)\right] \right. \\
&\quad \left. - \frac{\alpha_s^3 [4(128N_f + 1008\ln(2) - 19509) + 192(N_f - 9)\ln(\frac{\mu^2}{4m_Q^2}) + 7263\pi^2]}{1620m_Q^6} \right\} \langle \mathcal{O}(^1D_2^{[1]}) \rangle_{LO},
\end{aligned} \tag{27d}$$

where the states  $|Q\bar{Q}[n]\rangle$  in the l.h.s. and the r.h.s. should be understood to have been normalized under the same condition. Moreover, the equalities in (27) are independent on the normalization conventions. That is, the state  $|Q\bar{Q}[n]\rangle$  can be normalized either relativistically or non-relativistically, either as a composite state or as a discrete state. Therefore it is convenient to use  $\text{Im}\mathcal{A}$  to do the matching calculations, and we will use the abbreviation  $\text{Im}\mathcal{A}(n)$  to represent the amplitudes in (27).

The remaining infrared divergences and Coulomb singularities in (27) will be precisely repeated in the radiative corrections of the matrix elements in perturbative NRQCD in next section. The finite short distance coefficients will be obtained after matching calculations.

#### IV. NRQCD RESULTS AND OPERATOR EVOLUTION EQUATIONS

In this section, we calculate the NRQCD corrections to the four fermion operators in D dimensions. As we have mentioned, we will adopt the method of regions [19] to avoid the mismatch of the loop momenta in different regions. Furthermore, each loop integral in this method contributes only to a single power in  $v$ , thus one can do the power counting before the integral has been explicitly done.

Since the ultrasoft and the QCD scale are comparable,  $m_Q v^2 \sim \Lambda_{QCD}$ , for both charmonium and bottomonium, there are only two low-energy scales to be considered in NRQCD, which satisfy the inequality  $m_Q v \gg m_Q v^2$ . Thus, the nontrivial contributions to the

$$\begin{aligned}
\text{soft :} \quad Q_s : & \xrightarrow{(T, \vec{p})} = \frac{i}{T+i\epsilon}, \quad \vec{A}_s : \xrightarrow{i \quad k \quad j} = \frac{i\delta_{tr}^{ij}}{k^2+i\epsilon} \\
\text{potential :} \quad Q_p : & \xrightarrow{(T, \vec{p})} = \frac{i}{T-\frac{\vec{p}^2}{2m_Q}+i\epsilon}, \\
A_{p,0} : & \text{-----} = \frac{-i}{-k^2+i\epsilon}, \quad \vec{A}_p : \text{-----} = \frac{i\delta_{tr}^{ij}}{-k^2+i\epsilon}, \\
\text{ultrasoft :} \quad \vec{A}_u : & \xrightarrow{\sim} = \frac{i\delta_{tr}^{ij}}{k^2+i\epsilon}.
\end{aligned}$$

FIG. 5: NRQCD Feynman rules for heavy quark and gluon propagators in different regions

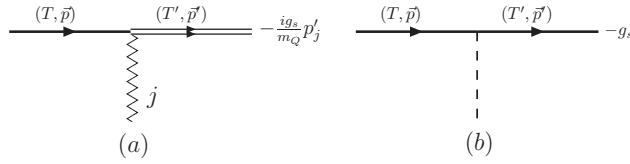


FIG. 6: NRQCD Feynman rules for heavy quark and gluon vertices

NRQCD loop integrals come only from the following three regions:

$$\begin{aligned}
\text{soft :} \quad A_s^\mu : \quad k_0 & \sim |\vec{k}| \sim m_Q v, \quad \Psi_s : T \sim |\vec{p}| \sim m_Q v, \\
\text{potential :} \quad A_p^\mu : \quad k_0 & \sim m_Q v^2, |\vec{k}| \sim m_Q v, \quad \Psi_p : T \sim m_Q v^2, |\vec{p}| \sim m_Q v, \\
\text{ultrasoft :} \quad A_u^\mu : \quad k_0 & \sim |\vec{k}| \sim m_Q v^2,
\end{aligned} \tag{28}$$

where  $k_\nu$  and  $p_\nu$  are the momenta of gluon field and heavy quark field respectively and  $T = p_0 - m_Q$ . The loop momenta running in these regions scale as those of the corresponding gluons in dimensional regularization scheme. One can check that the other regions, such as that with  $k_0 \sim m_Q v$  and  $\vec{k} \sim m_Q v^2$ , have no contributions to the NRQCD loop integrals in dimensional regularization scheme. In the view point of effective field theory, the five modes defined in (28) can be all treated as the effective fields in NRQCD. Only after parting these low-energy modes sufficiently like what has been done in (28), the homogeneous power counting rules can be gotten.

In practice, we use the NRQCD Feynman rules [34] derived in Coulomb gauge for the three regions (or the five low-energy modes) in our calculations. These rules are shown in Fig. 5 and 6, where  $\delta_{tr}^{ij} = \delta^{ij} - \frac{k^i k^j}{|\mathbf{k}|^2}$ . The Feynman rules for anti-heavy quark could be obtained by charge conjugation symmetry.



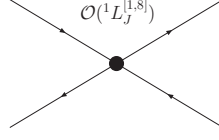


FIG. 7: NRQCD Feynman diagrams for LO Matrix Elements

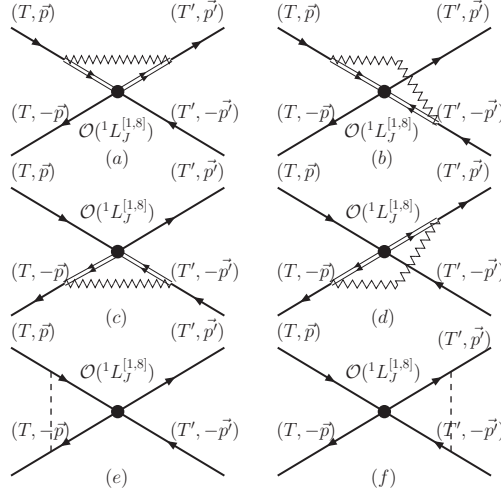


FIG. 8: NRQCD Feynman diagrams for NLO Matrix Elements

The Coulomb singularities calculated in full QCD theory correspond to the potential region, while the soft divergences to the soft one. The LO Feynman diagrams for matrix elements are shown in Fig. 7. The onshell external quark lines lie in potential region. At NLO in  $\alpha_s$ , only six classes of Feynman diagrams shown in Fig. 8 need to be calculated for our purpose [8]. The first four diagrams (a)-(d) have inner gluon lines connecting with one incoming quark line and one outgoing quark line, and the soft region will give the lowest order nontrivial result in  $v$  [8]. In the last two diagrams (e) and (f) the inner gluon line joints two incoming or outgoing quark lines, and only the potential region has non-vanishing real value [8]. The self-energy diagrams in the external legs are dropped in accordance with the on-shell renormalization scheme used in the full QCD calculation.

We present here the detailed calculation of the NLO correction to the P-wave octet operator  $\mathcal{O}(^1P_1^{[8]})$ . The LO result  $\langle \mathcal{O}(^1P_1^{[8]}) \rangle_{\text{Born}}$  is trivial. Using the Feynman rules for propagators of heavy quark and gluon in soft region and for the heavy quark gluon vertex

between potential and soft regions, the loop integral of diagram (a) is:

$$I_a = \frac{ig_s^2}{m_Q^2} \int \frac{d^D k}{(2\pi)^D} \frac{\mathbf{p} \cdot \mathbf{p}' - (\mathbf{p} \cdot \mathbf{k})(\mathbf{p}' \cdot \mathbf{k})/\mathbf{k}^2}{k_0^2 - \mathbf{k}^2 + i\epsilon} \frac{1}{k_0 - i\epsilon} \frac{1}{k_0 - i\epsilon}. \quad (29)$$

After performing the contour-integration of  $k_0 = |\mathbf{k}| - i\epsilon$ , we get<sup>b</sup>

$$I_a = \frac{g_s^2}{2m_Q^2} \int \frac{d^{D-1} k}{(2\pi)^{D-1}} \frac{\mathbf{p} \cdot \mathbf{p}' - (\mathbf{p} \cdot \mathbf{k})(\mathbf{p}' \cdot \mathbf{k})/\mathbf{k}^2}{|\mathbf{k}|^3}, \quad (30)$$

which is both infrared and ultraviolet divergent. The integral in (30) is scaleless, so vanishes in dimensional regularization. That is, the UV pole will be canceled by the IR one. But the result is nontrivial:

$$I_a = \frac{\alpha_s}{3\pi m_Q^2} \left( \frac{1}{\epsilon_{UV}} - \frac{1}{\epsilon} \right) \mathbf{p} \cdot \mathbf{p}'. \quad (31)$$

The integrals of (b)-(d) in Fig. 8 could be evaluated in the same way, and their results are:

$$I_{b-d} = \frac{\alpha_s}{3\pi m_Q^2} \left( \frac{1}{\epsilon_{UV}} - \frac{1}{\epsilon} \right) \mathbf{p} \cdot \mathbf{p}'. \quad (32)$$

Making use of the Feynman rules for heavy quarks and gluon in potential region, we obtain the loop integral of diagram (e):

$$I_e = -ig_s^2 \int \frac{d^D k}{(2\pi)^D} \frac{1}{\mathbf{k}^2} \frac{1}{T + k_0 - \frac{(\mathbf{p}+\mathbf{k})^2}{2m_Q} + i\epsilon} \frac{1}{T - k_0 - \frac{(\mathbf{p}+\mathbf{k})^2}{2m_Q} + i\epsilon}, \quad (33)$$

where  $T = \frac{|\mathbf{p}|^2}{2m_Q}$ . Integrating  $k_0$ , we have

$$I_e = g_s^2 m_Q \int \frac{d^{D-1} k}{(2\pi)^{D-1}} \frac{1}{\mathbf{k}^2} \frac{1}{\mathbf{k}^2 + 2\mathbf{p} \cdot \mathbf{k} - i\epsilon}. \quad (34)$$

This integral could be performed directly by introducing  $v = \frac{|\mathbf{p}|}{m_Q}$ , and we get the Coulomb singularity:

$$I_e = \frac{\alpha_s \pi}{4v} \left( 1 - \frac{i}{\pi} \left( \frac{1}{\epsilon} - \ln \left( \frac{m_Q^2 v^2}{\pi \mu^2} \right) - \gamma_E \right) \right). \quad (35)$$

The integral of diagram (f) gives the same Coulomb singularity but with opposite sign in the imaginary part.

---

<sup>b</sup> Since the quark propagator poles should be taken into account in the potential region, one only needs to evaluate the contribution from the gluon pole in the soft region [19].

The color structures of diagrams (a,c), (b,d) and (e,f) are obtained by color decomposition and are listed below respectively:

$$\begin{aligned}
\sqrt{2}T^a T^b \otimes T^b \sqrt{2}T^a &= C_F \frac{1}{\sqrt{3}} \otimes \frac{1}{\sqrt{3}} + \frac{N_c^2 - 2}{2N_c} \sqrt{2}T^c \otimes \sqrt{2}T^c, \\
\sqrt{2}T^a T^b \otimes \sqrt{2}T^a T^b &= C_F \frac{1}{\sqrt{3}} \otimes \frac{1}{\sqrt{3}} + \frac{-2}{2N_c} \sqrt{2}T^c \otimes \sqrt{2}T^c, \\
T^b \sqrt{2}T^a T^b \otimes \sqrt{2}T^a &= (C_F - \frac{1}{2}C_A) \sqrt{2}T^c \otimes \sqrt{2}T^c.
\end{aligned} \tag{36}$$

Summing over each integral multiplied by the according color factor we get NRQCD matrix element of P-wave operator at NLO, which is UV divergent and needs to be renormalized:

$$\begin{aligned}
\langle \mathcal{O}^0(^1P_1^{[8]}) \rangle_{NLO} &= \{ (1 + \frac{\alpha_s \pi}{2v} (C_F - \frac{1}{2}C_A)) \sqrt{2}T^c \otimes \sqrt{2}T^c + \\
&\frac{4\alpha_s (\frac{\mu}{\mu_\Lambda})^{2\epsilon}}{3\pi m_Q^2} (\frac{1}{\epsilon_{UV}} - \frac{1}{\epsilon}) [C_F \frac{1}{\sqrt{3}} \otimes \frac{1}{\sqrt{3}} + B_F \sqrt{2}T^c \otimes \sqrt{2}T^c] \mathbf{p} \cdot \mathbf{p}' \} \langle \bar{\mathcal{O}}(^1P_1) \rangle_{LO},
\end{aligned} \tag{37}$$

where we have used  $\langle \mathcal{O}^0(^1P_1^{[8]}) \rangle = \langle \bar{\mathcal{O}}(^1P_1) \rangle \sqrt{2}T^a \otimes \sqrt{2}T^a$  and the superscript 0 means the bare operator. Before doing the operator renormalization, we first re-express the bare result as

$$\begin{aligned}
\langle \mathcal{O}^0(^1P_1^{[8]}) \rangle_{NLO} &= (1 + \frac{\alpha_s \pi}{2v} (C_F - \frac{1}{2}C_A)) \langle \mathcal{O}(^1P_1^{[8]}) \rangle_{LO} \\
&+ \frac{4\alpha_s (\frac{\mu}{\mu_\Lambda})^{2\epsilon}}{3\pi m_Q^2} (\frac{1}{\epsilon_{UV}} - \frac{1}{\epsilon}) (C_F \langle \mathcal{O}(^1D_2^{[1]}) \rangle_{LO} + B_F \langle \mathcal{O}(^1D_2^{[8]}) \rangle_{LO}).
\end{aligned} \tag{38}$$

From the above equation we can see that the color-octet P-wave operator is mixed with the color-singlet D-wave operator at NLO in  $\alpha_s$ . We define the renormalized operator  $\mathcal{O}^R(^1P_1^{[8]})$  through [33]

$$\begin{aligned}
\langle \mathcal{O}^0(^1P_1^{[8]}) \rangle_{NLO} &= \langle \mathcal{O}^R(^1P_1^{[8]}) \rangle_{NLO} + \frac{4\alpha_s (\frac{\mu}{\mu_\Lambda})^{2\epsilon}}{3\pi m_Q^2} (\frac{1}{\epsilon_{UV}} + \ln 4\pi - \gamma_E) (C_F \langle \mathcal{O}(^1D_2^{[1]}) \rangle_{LO} \\
&+ B_F \langle \mathcal{O}(^1D_2^{[8]}) \rangle_{LO}).
\end{aligned} \tag{39}$$

Here the  $\overline{MS}$  renormalization scheme is adopted. The matrix element of the renormalized operator is UV finite, but still has IR divergence term which will cancel the infrared divergent D-wave full QCD result. And it also has the Coulomb singularity, which is the same as that appearing in the full QCD virtual correction:

$$\begin{aligned}
\langle \mathcal{O}^R(^1P_1^{[8]}) \rangle_{NLO} &= (1 + \frac{\alpha_s \pi}{2v} (C_F - \frac{1}{2}C_A)) \langle \mathcal{O}(^1P_1^{[8]}) \rangle_{LO} \\
&+ \frac{4\alpha_s (\frac{\mu}{\mu_\Lambda})^{2\epsilon}}{3\pi m_Q^2} (-\frac{1}{\epsilon} - \ln 4\pi + \gamma_E) (C_F \langle \mathcal{O}(^1D_2^{[1]}) \rangle_{LO} + B_F \langle \mathcal{O}(^1D_2^{[8]}) \rangle_{LO}).
\end{aligned} \tag{40}$$

Here, the matrix element of  $\mathcal{O}(^1D_2^{[8]})$  is at higher order in  $v$  in our case and therefore can be eliminated. The matrix elements of S-wave singlet and octet operators and that of the

D-wave singlet operator could be computed in the same way:

$$\begin{aligned} \langle \mathcal{O}^R(^1S_0^{[1]}) \rangle_{NLO} &= (1 + \frac{\alpha_s \pi}{2v} C_F) \langle \mathcal{O}(^1S_0^{[1]}) \rangle_{LO} \\ &+ \frac{1}{2N_c} \frac{4\alpha_s (\frac{\mu}{\mu_\Lambda})^{2\epsilon}}{3\pi m_Q^2} (-\frac{1}{\epsilon} - \ln 4\pi + \gamma_E) \langle \mathcal{O}(^1P_1^{[8]}) \rangle_{LO}, \end{aligned} \quad (41)$$

$$\begin{aligned} \langle \mathcal{O}^R(^1S_0^{[8]}) \rangle_{NLO} &= (1 + \frac{\alpha_s \pi}{2v} (C_F - \frac{1}{2}C_A)) \langle \mathcal{O}(^1S_0^{[8]}) \rangle_{LO} \\ &+ B_F \frac{4\alpha_s (\frac{\mu}{\mu_\Lambda})^{2\epsilon}}{3\pi m_Q^2} (-\frac{1}{\epsilon} - \ln 4\pi + \gamma_E) \langle \mathcal{O}(^1P_1^{[8]}) \rangle_{LO} + \dots, \end{aligned} \quad (42)$$

$$\langle \mathcal{O}^R(^1D_2^{[1]}) \rangle_{NLO} = (1 + \frac{\alpha_s \pi}{2v} C_F) \langle \mathcal{O}(^1D_2^{[1]}) \rangle_{LO} + \dots, \quad (43)$$

where "..." denotes terms at higher order in  $v$ .

Finally combining the matrix elements given above with the short distance coefficients accordingly, we get the forward scattering amplitudes for  $^1L_J$  states computed by NRQCD effective theory, which are summarized below:

$$(2\text{Im}\mathcal{A}(^1S_0^{[1]})) \Big|_{\text{pert NRQCD}} = \frac{2\text{Im}f(^1S_0^{[1]})}{m_Q^2} (1 + C_F \frac{\alpha_s \pi}{2v}) \langle \mathcal{O}(^1S_0^{[1]}) \rangle_{LO}, \quad (44a)$$

$$(2\text{Im}\mathcal{A}(^1S_0^{[8]})) \Big|_{\text{pert NRQCD}} = \frac{2\text{Im}f(^1S_0^{[8]})}{m_Q^2} [1 + (C_F - \frac{1}{2}C_A) \frac{\alpha_s \pi}{2v}] \langle \mathcal{O}(^1S_0^{[8]}) \rangle_{LO}, \quad (44b)$$

$$\begin{aligned} (2\text{Im}\mathcal{A}(^1P_1^{[8]})) \Big|_{\text{pert NRQCD}} &= \left\{ \frac{2\text{Im}f(^1P_1^{[8]})}{m_Q^4} [1 + (C_F - \frac{1}{2}C_A) \frac{\alpha_s \pi}{2v}] \right. \\ &\left. - \frac{1}{2N_c} \frac{4\alpha_s}{3\pi m_Q^4} \frac{2\text{Im}f(^1S_0^{[1]})}{\epsilon} - \frac{4\alpha_s B_F}{3\pi m_Q^4} \frac{2\text{Im}f(^1S_0^{[8]})}{\epsilon} \right\} \langle \mathcal{O}(^1P_1^{[8]}) \rangle_{LO}, \end{aligned} \quad (44c)$$

$$\begin{aligned} (2\text{Im}\mathcal{A}(^1D_2^{[1]})) \Big|_{\text{pert NRQCD}} &= \left[ \frac{2\text{Im}f(^1D_2^{[1]})}{m_Q^6} (1 + C_F \frac{\alpha_s \pi}{2v}) \right. \\ &\left. - \frac{4\alpha_s C_F}{3\pi m_Q^6} \frac{2\text{Im}f(^1P_1^{[8]})}{\epsilon} \right] \langle \mathcal{O}(^1D_2^{[1]}) \rangle_{LO}. \end{aligned} \quad (44d)$$

Setting expressions in (44) equal to those in (27) respectively, and expanding  $\text{Im}f_n$  in power of  $\alpha_s$ , we obtain the IR finite short distance coefficients up to  $\mathcal{O}(\alpha_s^3)$ :

$$2\text{Im}f(^1S_0^{[1]}) = \frac{8\pi\alpha_s^2}{3} + \frac{\alpha_s^3}{27} (4(477 - 16N_f) + 12(33 - 2N_f) \ln(\frac{\mu^2}{4m_Q^2}) - 93\pi^2), \quad (45a)$$

$$2\text{Im}f(^1S_0^{[8]}) = \frac{5\pi\alpha_s^2}{6} + \frac{5\alpha_s^3}{432} (16(153 - 4N_f) + 12(33 - 2N_f) \ln(\frac{\mu^2}{4m_Q^2}) - 129\pi^2), \quad (45b)$$

$$2\text{Im}f(^1P_1^{[8]}) = \frac{\pi\alpha_s^2}{2} + \frac{\alpha_s^3}{108}\{-3(6N_f - 61)\ln(\frac{\mu^2}{4m_Q^2}) + 2[-(24N_f + 63\ln(2) + 725) + 119\pi^2 + 114\ln(\frac{\mu}{\mu_\Lambda})]\}, \quad (45c)$$

$$2\text{Im}f(^1D_2^{[1]}) = \frac{16\pi\alpha_s^2}{45} + \frac{\alpha_s^3}{1620}[78720 - 512N_f - 7263\pi^2 - 4032\ln(2) + 2880\ln(\frac{\mu}{\mu_\Lambda}) - 192(N_f - 9)\ln(\frac{\mu^2}{4m_Q^2})], \quad (45d)$$

where the short distance coefficients of P-wave and D-wave are  $\mu_\Lambda$ -dependent. Their  $\mu_\Lambda$ -dependence will be canceled by that of the corresponding renormalized operators, which could be obtained by finding the derivative of both sides of (40,41,42) of  $\mu_\Lambda$ . For Born quantities,  $\frac{d\langle\mathcal{O}(^1L_J^{[1,8]})\rangle_{LO}}{d\mu_\Lambda} = 0$ . Then we obtain the renormalization group equations at leading order in  $v$  and  $\alpha_s$ :

$$\begin{aligned} \frac{d\langle\mathcal{O}^R(^1P_1^{[8]})\rangle_{NLO}}{d\ln\mu_\Lambda} &= \frac{8\alpha_s C_F}{3\pi m_Q^2} \langle\mathcal{O}(^1D_2^{[1]})\rangle_{LO}, \\ \frac{d\langle\mathcal{O}^R(^1S_0^{[1]})\rangle_{NLO}}{d\ln\mu_\Lambda} &= \frac{1}{2N_c} \frac{8\alpha_s}{3\pi m_Q^2} \langle\mathcal{O}(^1P_1^{[8]})\rangle_{LO}, \\ \frac{d\langle\mathcal{O}^R(^1S_0^{[8]})\rangle_{NLO}}{d\ln\mu_\Lambda} &= \frac{8\alpha_s B_F}{3\pi m_Q^2} \langle\mathcal{O}(^1P_1^{[8]})\rangle_{LO}. \end{aligned} \quad (46)$$

The solutions of the matrix elements  $\langle^1D_2|\mathcal{O}(\mu_\Lambda)|^1D_2\rangle$  in heavy quarkonium D-wave state  $^1D_2$  are:

$$\begin{aligned} \langle^1D_2|\mathcal{O}^R(^1P_1^{[8]})(\mu_\Lambda)|^1D_2\rangle &= \frac{8C_F}{3m_Q^2 b_0} \ln \frac{\alpha_s(\mu_{\Lambda_0})}{\alpha_s(\mu_\Lambda)} \langle^1D_2|\mathcal{O}(^1D_2^{[1]})|^1D_2\rangle, \\ \langle^1D_2|\mathcal{O}^R(^1S_0^{[1]})(\mu_\Lambda)|^1D_2\rangle &= \frac{C_F}{4N_c} \left(\frac{8}{3m_Q^2 b_0} \ln \frac{\alpha_s(\mu_{\Lambda_0})}{\alpha_s(\mu_\Lambda)}\right)^2 \langle^1D_2|\mathcal{O}(^1D_2^{[1]})|^1D_2\rangle, \\ \langle^1D_2|\mathcal{O}^R(^1S_0^{[8]})(\mu_\Lambda)|^1D_2\rangle &= \frac{C_F B_F}{2} \left(\frac{8}{3m_Q^2 b_0} \ln \frac{\alpha_s(\mu_{\Lambda_0})}{\alpha_s(\mu_\Lambda)}\right)^2 \langle^1D_2|\mathcal{O}(^1D_2^{[1]})|^1D_2\rangle, \end{aligned} \quad (47)$$

where the initial matrix elements like  $\langle^1D_2|\mathcal{O}^R(^1P_1^{[8]})(\mu_{\Lambda_0})|^1D_2\rangle$  at  $\mu_{\Lambda_0} = m_Q v$  are eliminated at LO in  $v$  [1, 8].

## V. NUMERICAL RESULTS AND PHENOMENOLOGICAL DISCUSSIONS

The long distance matrix element of D-wave four-fermion color-singlet operator in the hadron state is related with the second derivative of radial wave function at the origin

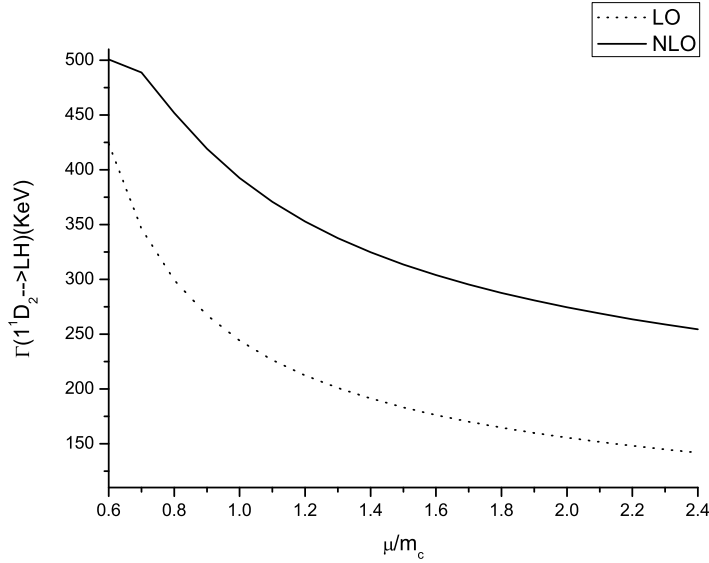


FIG. 9: Renormalization scale dependence of the decay width of charmonium state  $1^1D_2$  to LH

through the following relation:

$$\langle n^1D_2 | \mathcal{O}(n^1D_2) | n^1D_2 \rangle = \frac{15|R''_{nD}(0)|^2}{8\pi} = m_Q^6 H_{Dn} . \quad (48)$$

Combining the leading order coefficient  $2\text{Im}f(^1D_2^{[1]})_{LO} = 16\pi\alpha_s^2/45$  given in (45d) and the color-singlet matrix element given in (48), one can reproduce the decay width of  $^1D_2$  state in the CSM at leading order in  $\alpha_s$  [10]:

$$\Gamma_{CSM}(n^1D_2 \rightarrow gg) = \frac{2\alpha_s^2}{3} \frac{|R''_{nD}(0)|^2}{m_Q^6} . \quad (49)$$

However, there are contributions from the color-octet Fock states in (7) in NRQCD even at the order of  $\alpha_s^2$ . The matrix elements of the P-wave octet operator and S-wave singlet as well as octet operators in the  $^1D_2$  bound state could be estimated through the solutions of the operator evaluation equations in (47).

The region of validity of the evolution equation is chosen as follows: the lower limit  $\mu_{\Lambda_0} = m_Q v$  and the upper limit  $\mu_{\Lambda}$  of order  $m_Q$ . For convenience, we take the factorization scale  $\mu_{\Lambda}$  to be the same as the renormalization scale  $\mu$  of order  $m_Q$ . We choose the pole mass  $m_c = 1.5\text{GeV}$ ,  $v^2 = 0.3$ ,  $\mu_{\Lambda_0} = m_c v$ ,  $\mu_{\Lambda} = 2m_c$ ,  $\alpha_s(2m_c) = 0.249$ ,  $N_f = 3$ ,  $\Lambda_{QCD} = 390\text{MeV}$ ,  $H_{D1} = \frac{15|R'_{1D}(0)|^2}{8\pi m_c^6} = 0.786 \times 10^{-3}\text{GeV}$  [35] for charmonium, and  $m_b = 4.6\text{GeV}$ ,  $v^2 = 0.1$ ,  $\mu_{\Lambda_0} = m_b v$ ,  $\mu_{\Lambda} = 2m_b$ ,  $\alpha_s(2m_b) = 0.180$ ,  $N_f = 4$ ,  $\Lambda_{QCD} = 340\text{MeV}$ ,  $H_{D1} = \frac{15|R'_{1D}(0)|^2}{8\pi m_b^6} = 0.401 \times 10^{-4}\text{GeV}$  for  $1D$  states and  $H_{D2} = \frac{15|R'_{2D}(0)|^2}{8\pi m_b^6} = 0.750 \times 10^{-4}\text{GeV}$  for  $2D$  states [35] for bottomonium. The  $\mu$  dependence curves of the decay widths are shown in Fig. 9 and Fig.

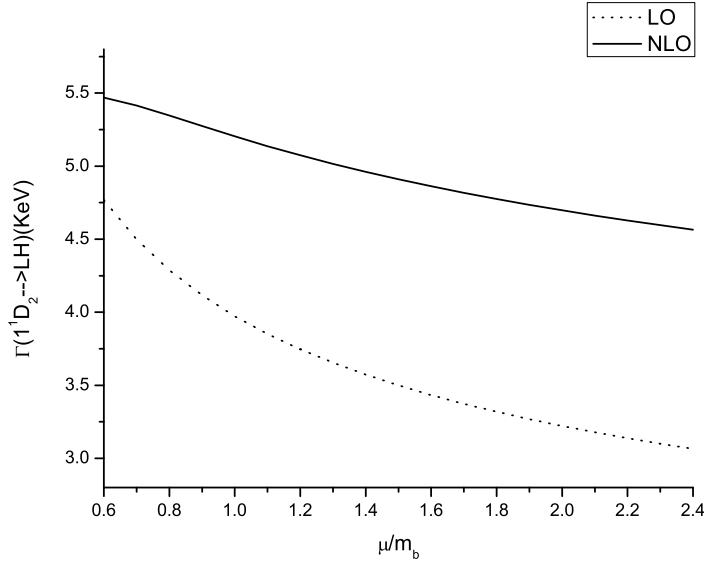


FIG. 10: Renormalization scale dependence of the decay width of bottomonium state  $1^1D_2$  to LH

TABLE V: Subprocess decay rates of  $1^1D_2$  charmonium, where  $m_c = 1.5\text{GeV}$ ,  $v^2 = 0.3$ ,  $\mu_{\Lambda_0} = m_c v$ ,  $\mu_\Lambda = 2m_c$  and  $\alpha_s(2m_c) = 0.249$ .

Subprocess	LO(KeV)	NLO(KeV)
$(^1D_2)_1 \rightarrow LH$	54.7	75.1
$(^1P_1)_8 \rightarrow LH$	66.6	132
$(^1S_0)_8 \rightarrow LH$	15.0	31.3
$(^1S_0)_1 \rightarrow LH$	19.2	36.1

10. When  $\mu = 2m_c$  for  $c\bar{c}$  systems and  $2m_b$  for  $b\bar{b}$  systems, we get the predictions at  $\mathcal{O}(\alpha_s^3)$ :

$$\begin{aligned}
\Gamma_C(1^1D_2 \rightarrow LH) &= 274\text{KeV}, \\
\Gamma_B(1^1D_2 \rightarrow LH) &= 4.70\text{KeV}, \\
\Gamma_B(2^1D_2 \rightarrow LH) &= 8.78\text{KeV}.
\end{aligned} \tag{50}$$

The LO decay widths for charmonium and bottomonium  $1^1D_2$  states are 155 KeV and 3.22 KeV. Therefore the NLO QCD corrections contribute enhancement of factor 1.8 and 1.5, respectively.

For the  $1^1D_2$  charmonium state  $\eta_{c2}$ , the numerical values for all subprocesses are also listed in Table V. One can see from this table that the contributions from the Fock states

other than  $|^1D_2^{[1]}\rangle$  are dominant in the decay width, and the total result is about 1-3 times larger than that in CSM even at leading order in  $\alpha_s$ .

For the phenomenological analysis of  $\eta_{c2}$ , we vary the renormalization/factorization scale from  $2m_c$  to  $m_c$  and get  $\Gamma(\eta_{c2} \rightarrow LH) = 274\text{-}392$  KeV. The electric transition rate  $\Gamma(\eta_{c2} \rightarrow \gamma h_c) = 339\text{-}375$  KeV [13] and the dipion transition rate  $\Gamma(\eta_{c2} \rightarrow \eta_c \pi \pi) \approx 45$  KeV [11] have been estimated elsewhere in the literature.

As emphasized before, the  $\eta_{c2}$  should be a narrow state, since its mass and quantum numbers forbid it to decay into charmed meson pairs  $D\bar{D}$  and  $D^*\bar{D}$ . Therefore, the main decays modes of  $\eta_{c2}$  are expected to be the electric as well as hadronic transitions to lower-lying charmonium states and the inclusive light hadronic decay. With all these decay widths given above, we get the total width of  $\eta_{c2}$  to be about 660-810 KeV, and the branching ratio of the electric transition to be

$$\mathcal{B}(\eta_{c2} \rightarrow \gamma h_c) = (44\text{-}54)\%, \quad (51)$$

which provides important information on probing this missing state. In practice, one can search for  $\eta_{c2}$  through the cascade decay  $\eta_{c2} \rightarrow \gamma h_c \rightarrow \gamma \gamma \eta_c \rightarrow \gamma \gamma K \bar{K} \pi$  with branching ratios  $\mathcal{B}(h_c \rightarrow \gamma \eta_c) \approx 0.4$  [11, 37] and  $\mathcal{B}(\eta_c \rightarrow K \bar{K} \pi) \approx 7\%$  [36]. Similar decay chains can also be used to search for the  $\eta_{b2}^{(\prime)}$ .

The production rates of  $\eta_{c2}$  are expected to be generally low in many processes, because the rates are suppressed by the small values of the second derivative of the wave function at the origin, and also by its spin-singlet nature, which forbids  $\eta_{c2}$  to couple to a photon, or to be detected from the E1 transitions of higher spin-triplet charmonia. Nevertheless, efforts should be made to find this very unique missing charmonium state. Hopefully, the study for the inclusive light hadronic decay of  $\eta_{c2}$  in NRQCD will provide useful information on searching for this state in high-energy  $p\bar{p}$  collision [14], in  $B$  decays [15], in higher charmonium transitions, in  $e^+e^-$  process in BESIII at BEPC [17], and particularly in the low-energy  $p\bar{p}$  reaction in PANDA at FAIR [16].

## VI. SUMMARY

In this paper, we calculate the inclusive light hadronic decay width of the  $^1D_2$  heavy quarkonium state up to order of  $\alpha_s^3$  and at the leading order in  $v$  within the framework of



NRQCD. We find that the inclusive decay widths into light hadrons via gluons and light quarks at order of  $\alpha_s^3$  in QCD suffer from both IR divergences and Coulomb singularities, but they can be absorbed into the renormalization of the matrix elements of the four-fermion operators in NRQCD precisely. Therefore, after matching the full QCD onto NRQCD, the IR divergent part is removed, and IR finite short-distant coefficients are obtained, and the dependence on the factorization scale of the coefficient is canceled by that of the corresponding matrix element with the renormalization group analysis.

At leading order in  $\alpha_s$ , the result in the CSM can be reproduced but there are many other contributions, such as that from color-octet P-wave operators, which will enhance the width in CSM by several times in magnitude even at the leading order in  $\alpha_s$ . Furthermore, the NLO results give extra enhancement factors of 1.8 for  $\eta_{c2}$  and 1.5 for  $\eta_{b2}$  relative to the LO ones, respectively. By choosing the factorization scale as  $2m_Q$ , the light hadronic decay widths are found to be about 274, 4.7, and 8.8 KeV for the  $\eta_{c2}$ ,  $\eta_{b2}$ , and  $\eta'_{b2}$  respectively. Based on these estimates, and using the E1 transition width and dipion transition width for the  $\eta_{c2}$  estimated elsewhere in the literature, we get the total width of  $\eta_{c2}$  to be about 660-810 KeV, and the branching ratio of the electric transition  $\eta_{c2} \rightarrow \gamma h_c$  to be about (44-54)%, which will be useful in searching for this missing charmonium state through, e.g., the process  $\eta_{c2} \rightarrow \gamma h_c$  followed by  $h_c \rightarrow \gamma \eta_c$ .

## VII. ACKNOWLEDGEMENT

Y.F. would like to thank Dr. Ce Meng and Dr. Yu-Jie Zhang for useful discussion and reading the manuscript. Y.F. would also like to thank Mr. Rolf Mertig and Prof. Fabio Maltoni for their useful suggestions by e-mail. Z.G.H. thanks Institute of High Energy Physics of Chinese Academy of Sciences and Theoretical Physics Center for Science Facilities for their hospitality. This work was supported in part by the National Natural Science Foundation of China (No 10675003, No 10721063).

---

[1] G.T. Bodwin, E. Braaten, and G.P. Lepage, Phys. Rev. **D51**, 1125 (1995); *ibid.***D55**, 5853(E) (1997) (hep-ph/9407339).

- [2] See, e.g., J.H. Kühn, J. Kaplan, and E.G.O. Sadiani, Nucl. Phys. **B 157**, 125 (1979); C.H. Chang, Nucl. Phys. **B172**, 425 (1980); W.Y. Keung, Phys. Rev. **D 23**, 2072 (1981); J.H. Kühn and H. Schneider, Phys. Rev. **D 24**, 2996 (1981); L. Clavelli, Phys. Rev. **D26**, 1610 (1982).
- [3] G.T. Bodwin, E. Braaten, T.C. Yuan and G.P. Lepage, Phys. Rev. **D46** 3703 (1992) (hep-ph/9208254).
- [4] Han-Wen Huang and Kuang-Ta Chao, Phys. Rev. **D54**, 3065 (1996) ; *ibid.* **D56**, 7472(E) (1997) ; *ibid.* **D60**, 079901(E) (1999) (hep-ph/9601283).
- [5] Han-Wen Huang and Kuang-Ta Chao, Phys. Rev. **D55**, 244 (1997) (hep-ph/9605362).
- [6] Han-Wen Huang and Kuang-Ta Chao, Phys. Rev. **D54**, 6850 (1996) ; *ibid.* **D56**, 1821(E) (1997) (hep-ph/9606220).
- [7] Zhi-Guo He, Ying Fan and Kuang-Ta Chao, Phys. Rev. Lett. 101, 112001 (2008) (arXiv: 0802.1849).
- [8] Zhi-Guo He, Ying Fan and Kuang-Ta Chao, in preparation.
- [9] G. Belanger and P. Moxhay, Phys. Lett. **B199**, 575 (1987); L. Bergstrom and P. Ernststrom, Phys. Lett. **B267**, 111 (1991).
- [10] V.A. Novikov et al., Phys. Rept. **41**, 1 (1978).
- [11] Estia J.Eichten, Kenneth Lane and Chris Quigg, Phys. Rev. Lett. 89, 162002 (2002) (hep-ph/0206018).
- [12] E.J. Eichten, K. Lane and C. Quigg, Phys. Rev. **D69**, 094019 (2004) (hep-ph/0401210).
- [13] T. Barnes, S. Godfrey and E.S. Swanson, Phys. Rev. **D72**, 054026, (2005) (hep-ph/0505002); B.Q. Li and K.T. Chao, in preparation.
- [14] Frank Close, Phys. Lett. **B342**, 369 (1995) (hep-ph/9409203); Peter L. Cho and Mark B. Wise, Phys. Rev. **D51**, 3352 (1995) (hep-ph/9410214).
- [15] Pyungwon Ko, Jungil Lee and H.S. Song, Phys. Lett. **B395**, 107 (1997) (hep-ph/9701235); F. Yuan, C.F. Qiao and K.T. Chao, Phys. Rev. **D56**, 329 (1997) (hep-ph/9701250).
- [16] J. Ritman (for the PANDA collaboration), hep-ex/0702013.
- [17] D.M. Asner et al., arXiv: 0809.1869
- [18] A.V. Manohar, Phys. Rev. **D56**, 230 (1997) (hep-ph/9701294)
- [19] M.Beneke and V.A.Smirnov, Nucl. Phys. **B522**, 321 (1998) (hep-ph/9711391).
- [20] A.Petrelli, M.Cacciari, M.Greco, F.Maltoni and M.L.Mangano, Nucl. Phys. **B514**, 245 (1998)

- (hep-ph/9707223).
- [21] F.Maltoni. Quarkonium Phenomenology. Ph.D.thesis, 1998-'99.
  - [22] G.'t Hooft and M.Veltman, Nucl. Phys. **B44**, 189 (1972).
  - [23] J.Novotny, Czech. J. Phys, **44**, 633 (1994).
  - [24] R.Mertig and W.L.van Neerven, Z. Phys. **C70**, 637 (1996) (hep-ph/9506451).
  - [25] D.Kreimer, hep-ph/9401354.
  - [26] S.A.Larin, Phys. Lett. **B303**, 113 (1993) (hep-ph/9302240).
  - [27] P.Breitenlohner and D.Maison, Commun. Math. Phys. **52**, 11 (1977); **52**, 39 (1977); **52**, 55 (1977).
  - [28] G.T. Bodwin and A. Petrelli, Phys. Rev. **D66**, 094011 (2002) [hep-ph/0205210].
  - [29] R.Ticciati, *Quantum Field Theory For Mathematicians*, (Cambridge University Press, United Kingdom, 1999).
  - [30] Wai-Yee Keung and I.J.Muzinich, Phys. Rev. **D27**, 1518 (1983).
  - [31] M.Böhm, A.Denner, J.Küblbeck, Comput. Phys. Commun. **60** (1990) 165; T.Hahn, Comput. Phys. Commun. **140**, 418 (2001).
  - [32] R.Mertig, M.Böhm, A.Denner, Comput. Phys. Commun. 64 (1991) 345.
  - [33] M.Klasen, B.A.Kniehl, L.N.Mihaila and M.Steinhauser, Nucl. Phys. **B713**, 487 (2005).
  - [34] Harald W. Griesshammer, hep-ph/9804251.
  - [35] Estia J.Eichten and Chris Quigg, Phys. Rev. **D52**, 1726 (1995) (hep-ph/9503356).
  - [36] C.Amsler *et al.* [Particle Data Group], Phys. Lett. B **667**, 1 (2008).
  - [37] K.T. Chao, Y.B. Ding and D.H. Qin, Phys. Lett. B301, 282 (1993).